



Universidad Autónoma
de Madrid

Biblos-e Archivo
Repositorio Institucional UAM

Repositorio Institucional de la Universidad Autónoma de Madrid

<https://repositorio.uam.es>

Esta es la **versión de autor** del artículo publicado en:
This is an **author produced** version of a paper published in:

Hypertension 79.7 (2022): 1361-1373

DOI: <https://doi.org/10.1161/HYPERTENSIONAHA.121.18477>

Copyright: © American Heart Association, Inc

El acceso a la versión del editor puede requerir la suscripción del recurso

Access to the published version may require subscription

1 **Dipeptidyl peptidase-4 promotes human endothelial cell**
2 **senescence and dysfunction via PAR2-COX-2-TP axis and**
3 **NLRP3 inflammasome activation**

4
Inés Valencia^{1,2,3}, Susana Vallejo^{1,2}, Pilar Dongil^{1,2}, Alejandra Romero^{1,2}, Álvaro San Hipólito-Luengo^{1,2}, Licia Shamoon^{1,2,3}, María Posada⁴, Damián García-Olmo⁴, Raffaele Carraro^{5,6}, Jorge D. Erusalimsky⁷, Tania Romacho^{1,2}, Concepción Peiró^{1,2}, Carlos F. Sánchez-Ferrer^{1,2}.

¹Department of Pharmacology and Therapeutics, School of Medicine, Universidad Autónoma de Madrid, Madrid, Spain.

²Instituto de Investigación Sanitaria del Hospital Universitario La Paz (IdiPAZ), Madrid, Spain

³PhD Programme in Pharmacology and Physiology, Doctoral School, Universidad Autónoma de Madrid, Madrid, Spain.

⁴Service of Surgery and Instituto de Investigación Sanitaria del Hospital Fundación Jiménez Díaz, Madrid, Spain.

⁵Service of Endocrinology and Instituto de Investigación Sanitaria del Hospital Universitario La Princesa, Madrid, Spain.

⁶Department of Medicine, School of Medicine, Universidad Autónoma de Madrid, Madrid, Spain.

⁷School of Sport and Health Sciences, Cardiff Metropolitan University, Cardiff, UK.

Category: Original Article

Short title: sDPP4 triggers endothelial senescence and dysfunction

Word count: 7100 – MANUSCRIPT, REFERENCES, LEGENDS 8,162 ME SALEN
ESTAS

Abstract word count: 250

Number of figures: 6

Corresponding authors:

Carlos F. Sánchez-Ferrer, MD, PhD, Prof. carlosf.sanchezferrer@uam.es

Concepción Peiró, PhD, Prof. concha.peiro@uam.es

School of Medicine, Universidad Autónoma de Madrid

Department of Pharmacology and Therapeutics

Arzobispo Morcillo St. 28029 Madrid, Spain.

Phone: +34 91 497 5470

5 **Abstract**

6 Vascular aging is a multifaceted process characterized by structural modifications in
7 blood vessels, like the abnormal accumulation of senescent cells leading to a
8 compromised vascular function. Obesity and type 2 diabetes mellitus (T2DM) are
9 considered progeric conditions leading to premature vascular aging. Soluble dipeptidyl
10 peptidase 4 (sDPP4) secretion from adipose tissue (AT) is enhanced in obesity and
11 T2DM, where it was proven to mediate deleterious effects, albeit its contribution to
12 vascular aging is unknown. We aimed to explore sDPP4 involvement in vascular aging,
13 unravelling the molecular pathway by which sDPP4 acts on the endothelium. The present
14 study demonstrates that, by a common mechanism, sDPP4 triggers senescence in cultured
15 human endothelial cells and endothelial dysfunction in isolated human resistance arteries.
16 sDPP4 activates the metabotropic receptor PAR2, cyclooxygenase 2 (COX-2) activity
17 and the production of TXA₂ acting over TP receptors (PAR2-COX-2-TP axis), leading to
18 NLRP3 inflammasome activation. Additionally, in the pathological context of human
19 obesity, we explored some related parameters *in vitro* and *ex vivo*. Obese patients
20 exhibited impaired microarterial functionality in comparison to control non-obese
21 counterparts. Importantly, endothelial dysfunction in obese patients positively correlated
22 with greater expression of DPP4, pro-senescent, and pro-inflammatory markers in the
23 visceral AT nearby the resistance arteries. Moreover, when DPP4 activity or sDPP4-
24 induced pro-senescent mechanism were blocked, endothelial dysfunction was restored
25 back to levels of healthy subjects. These results reveal sDPP4 as a relevant mediator in
26 early vascular aging and highlight its capacity activating main pro-inflammatory
27 mediators in the endothelium that might be tackled with pharmacological tools.

28
29 **Keywords:** *dipeptidyl peptidase-4, endothelial senescence, endothelial dysfunction,*
30 *vascular aging, obesity. inflammaging, NLRP3 inflammasome.*

31

32

33

34

35

36

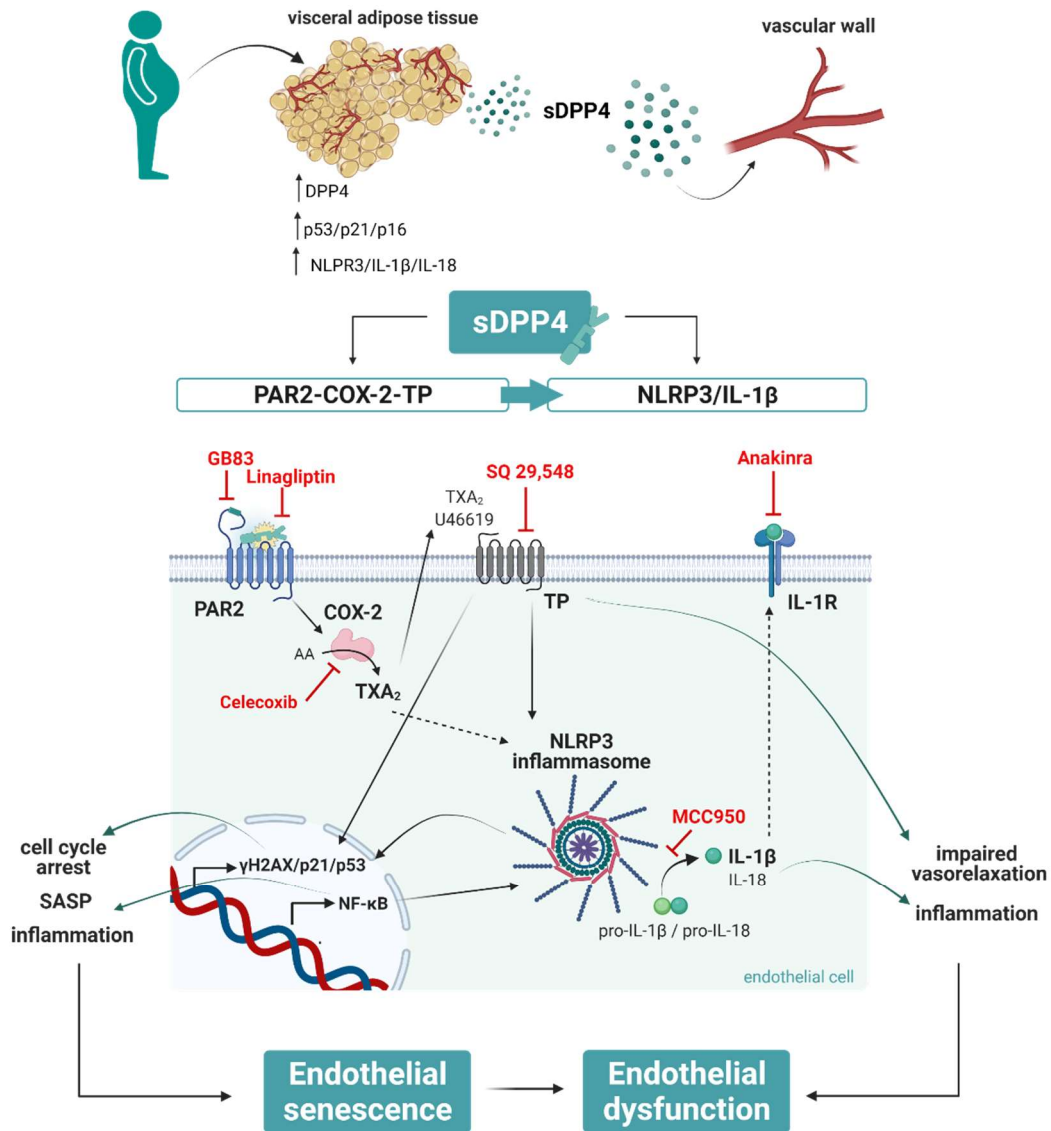
37

38

39

40
41
42

Graphical Abstract



43
44
45
46
47
48
49
50
51
52
53
54
55
56

Graphical abstract. Dipeptidyl peptidase-4 promotes human endothelial cell senescence and dysfunction via PAR2-COX-2-TP axis and NLRP3 inflammasome activation. Increased DPP4 release and expression in the context of obesity and other cardiometabolic diseases contributes to the inflammaging-prone microenvironment in which DPP4 can trigger endothelial cell senescence and endothelial dysfunction, contributing to further vascular disease. While DPP4 activates PAR2-COX-2-TP axis and NLRP3 inflammasome machinery, pharmacological inhibition of its enzymatic activity and downstream signalling prevents endothelial senescence and reverses endothelial dysfunction in a human model of obesity. DPP4 is an inducer of endothelial senescence and dysfunction and antidiabetic DPP4 inhibitors and other anti-inflammatory tools may entail therapeutic potential to delay vascular inflammaging and disease in cardiometabolic diseases.

57

58 **List of abbreviations**

59	ANOVA	Analysis of variance
60	ASC	Apoptosis-associated speck-like protein containing carboxyl-terminal CARD
61	AT	Adipose tissue
62	BK	Bradykinin
63	BMI	Body mass index
64	CMD	Cardiometabolic disease
65	COX-2	Cyclooxygenase-2
66	GIP	Gastric inhibitory polypeptide
67	GLP-1	Glucagon-like peptide-1
68	HUVEC	Human umbilical vein endothelial cells
69	IL	Interleukin
70	MCP-1	Monocyte chemoattractant protein 1
71	NLRP3	Nucleotide-binding oligomerization domain, leucine-rich repeat and pyrin
72		domain-containing-3
73	PAR2	Protease-activated receptor 2
74	SASP	Senescence-associated secretory phenotype
75	SA- β -gal	Senescence-associated β -galactosidase
76	SEM	Standard error of the mean
77	SNP	Sodium nitroprusside
78	TIFs	Telomere dysfunction-induced foci
79	TNF- α	Tumour necrosis factor
80	TP	Thromboxane receptor
81	TRF-1	Telomere repeat binding factor-1
82	TXA ₂	Thromboxane A ₂

83

84

85

86

87

88 **Introduction**

89 Vascular aging is a complex and multifaceted process that profoundly alters vascular
90 structure and functionality, predisposing to vascular diseases such as atherosclerosis and
91 endothelial dysfunction (1,2). Importantly, over the last years, cardiometabolic diseases
92 (CMD) such as obesity and type 2 diabetes mellitus, have been acknowledged as progeric
93 diseases exhibiting signs of premature vascular aging (3).

94 Endothelial senescence is the major process contributing to vascular aging (4). Cell
95 senescence is a cell irreversible state where a core of damage-sensing signalling pathways
96 is activated and cells lose their ability to divide while remaining metabolically active (5).
97 A causative relation between cellular senescence and endothelial dysfunction has been
98 demonstrated, as the progressive accumulation of endothelial senescent cells can induce
99 the dysregulation of vascular tone and arterial stiffening (4). Endothelial senescent cells
100 acquire a senescence-associated secretory phenotype (SASP) with pro-inflammatory,
101 pro-thrombotic and pro-atherogenic effects (6). The SASP profile in vascular endothelial
102 cells involves an enhanced release of mediators like tumour necrosis factor (TNF- α) and
103 chemokines and cytokines as monocyte chemoattractant protein 1 (MCP-1), interleukin-
104 (IL)-6 and IL-1 β , among others (7). This microenvironment contributes to an unresolved
105 and uncontrolled low-grade chronic inflammation that propagates the senescence
106 phenotype and exacerbates even more the aging process, named after the term
107 ‘inflammaging’ (8). Therefore, a better understanding of the molecular and physiological
108 basis of endothelial senescence is decisive to identify new therapeutic approaches to
109 tackle vascular aging.

110 Obesity is acknowledged as a chronic non-infectious disease that has reached epidemic
111 proportions globally, with about 2.5 million people dying annually as consequence of
112 being overweight or obese (9). The main characteristic of obesity is the enlargement and

113 inflammation of the adipose tissue (AT), currently recognized as a true endocrine organ.
114 The imbalanced secretion of active factors from AT, adipokines, towards a more pro-
115 atherogenic and pro-inflammatory phenotype, influences the local and systemic vascular
116 responses and contributes to vascular disease (10). In this pro-inflammatory context, the
117 innate immune response mediator nucleotide binding oligomerization domain, leucine-
118 rich repeat and pyrin domain-containing-3 (NLRP3) inflammasome have been proven as
119 a relevant contributor to the low-grade chronic inflammation underlying vascular disease
120 in obesity (11). AT is engaged in paracrine crosstalk with adjacent vascular trees (12)
121 and, therefore, not only perivascular AT but also visceral AT inflammation can modulate
122 the function of blood vessels in close proximity or even within the tissue.

123 Dipeptidyl peptidase 4 (DPP4) is a surface serine protease that can be shed from the
124 plasma membrane as a soluble form (sDPP4), recently identified among the substrates
125 released by the AT (13). Both the soluble and membrane-bound DPP4 cleaves N-terminal
126 dipeptides from diverse substrates like the incretin hormones glucagon-like peptide-1
127 (GLP-1) and gastric inhibitory polypeptide (GIP). The gliptin family of antidiabetic drugs
128 inhibit DPP4 activity, thus prolonging the half-life of incretins and glucose homeostasis
129 (14). Interestingly, sDPP4 plasma levels and activity are increased in type 2 diabetes
130 mellitus and obesity and they positively correlate with insulin resistance and an increased
131 risk score for the metabolic syndrome (13,15). Moreover, sDPP4 directly induces
132 inflammation in vascular cells and impair vasorelaxation in isolated murine microvessels
133 (16,17) by activating G-protein-coupled proteinase-activated receptors 2 (PAR2), which
134 are upregulated in animal models of obesity (18), and by triggering the activation of the
135 cyclooxygenase 2 (COX-2) and thromboxane receptor (TP) axis (16,17), namely the
136 PAR2-COX-2-TP axis. However, whether sDPP4 itself induces endothelial cell

137 senescence and thus contributes to premature vascular aging and endothelial dysfunction
138 is yet to be established.

139 In the search of new therapeutic targets to tackle accelerated vascular aging, we first
140 studied whether sDPP4 can directly induce cell senescence in cultured human endothelial
141 cells and endothelial dysfunction in human isolated mesenteric microvessels, while
142 exploring the underlying molecular pathway with focus on the PAR2-COX-2-TP axis and
143 NLRP3 inflammasome. We next determined DPP4 and pro-senescent markers expression
144 in visceral AT from control and obese patients and assessed the endothelial function of
145 the close microvasculature. Finally, we assessed whether gliptins or the pharmacological
146 blockade of sDPP4 downstream signalling pathways may improve the impaired reactivity
147 of microvessels from obese patients.

148

149 **Materials and Methods**

150 *Human umbilical vein endothelial cells (HUVEC) isolation and cell culture*

151 HUVEC were isolated from donated umbilical cords obtained in Hospital Universitario
152 La Paz (Madrid, Spain), with informed consent, following the Spanish legislation and
153 under approval of the appropriate Ethical Committee. Umbilical cord donors with CMD
154 were rejected. HUVEC were extracted by chemical digestion with 2 mmol/l type II
155 collagenase (Sigma, Saint Louis, Missouri, USA) and characterized by von-Willebrand
156 factor detection. Cells were cultured in supplemented M199 medium as previously
157 described (19).

158 *Collection of human omentum biopsies and health-associated parameters*

159 Omentum biopsies and basic blood analysis registers were obtained from a group of
160 patients (mean age 50 ± 13 years old, 57% male), classified as non-obese controls without

161 CMD (body mass index, $BMI < 30 \text{ kg}\cdot\text{m}^{-2}$) and obese patients ($BMI \geq 30 \text{ kg}\cdot\text{m}^{-2}$). All
162 procedures were approved by the Ethical Committee of Hospital Fundación Jiménez Díaz
163 (Madrid, Spain) and following the principles outlines in the Declaration of Helsinki. The
164 patients participating in the study were submitted to a non-urgent, non-septic abdominal
165 surgery consisting in cholecystectomies and bariatric surgery for control and obese
166 patients, respectively. After signature of an appropriate written consent, a 3 cm piece of
167 omentum was dissected during surgery and kept at 4°C until experimental use. Two
168 donors were dismissed from the experiments due to inappropriate manipulation of tissue
169 sample. Mesenteric arteries were obtained, cleaned, and mounted on a small vessel
170 myograph, while surrounding visceral AT was frozen immediately until total RNA
171 extraction was performed, as indicated below.

172 *Senescence Associated- β -galactosidase (SA- β -gal) assay*

173 SA- β -gal staining was performed following the prescriptions of a commercial kit from
174 Sigma, as previously described (20). The percentage of SA- β -gal positive cells over total
175 cells was determined by blind manual scoring of at least 2,000 cells per sample in 12
176 randomized fields, under an inverted microscope Nikon Eclipse TE300 (Tokyo, Japan)
177 connected to a Nikon DS-U3 camera and using the NIS-Element 4.50 imaging software,
178 in phase contrast mode with a 20X objective.

179 *Detection of γH2AX foci and telomere dysfunction-induced foci (TIFs) by double-* 180 *indirect immunofluorescence*

181 γH2AX foci representing DNA damage and TIFs, where γH2AX co-localizes with the
182 telomere protein telomere repeat binding factor-1 (TRF-1), were examined by indirect
183 double-immunofluorescence as described before (20). Samples were viewed under a
184 Nikon Eclipse 801 microscope connected to a Hamamatsu Orca 285 digital camera.
185 Fluorescence images were captured using the Volocity 3D image analysis software (Pekin

186 Elmers Inc., version 5.5). Z-stacks were converted to voxels (volume pixels) and further
187 analysed with the Volocity co-localization module after image projection. The average
188 fluorescence corresponding to each detected protein (expressed as voxels/cell) and the
189 percentage of TIFs-positive cells (considering cells with ≥ 5 γ H2AX-TRF-1 co-
190 localization sites), were determined by analysis of at least 200 nuclei in 10 random fields
191 per sample.

192 ***Western Blotting***

193 HUVEC were treated as indicated and lysed, while mechanically detached from the plate.
194 Protein content was quantified by a colorimetric protocol using the bicinchoninic acid
195 (BCA) method (Thermo Fisher Scientific, Illinois, USA). Thereafter, 20 μ g of protein
196 lysates were separated by SDS-PAGE electrophoresis and later transferred to polyvinyl
197 membranes (Merck, Darmstadt, Germany). Proteins were detected with primary
198 antibodies followed by corresponding horseradish peroxidase-labelled secondary
199 antibodies (please see <http://hyper.ahajournals.org>). Protein levels were normalized to β -
200 actin signal (Sigma). Immunoreactive bands were detected using an enhanced
201 chemiluminescence ECL detection kit (Bio-Rad, California, USA) and quantified by
202 densitometry using ImageJ 1.51w free software.

203 ***Determination of NLRP3 inflammasome activation by indirect immunofluorescence***

204 Apoptosis-associated speck-like protein containing carboxyl-terminal CARD (ASC)
205 specks were detected by incubation with primary anti-ASC antibody (Enzo Life Sciences,
206 New York, USA), followed by the secondary antibody Alexa Fluor 647-conjugated goat
207 anti-rabbit IgG (Jackson Immuno Research, Cambridge, UK). Nuclei were counterstained
208 with 1 μ mol/l 4'-6'-diamidino-2-phenylindole (DAPI). ASC specks per field were
209 quantified by manual blind scoring of 17 radial distributed fields in each sample, under

210 an inverted microscope Eclipse TE300 (Nikon). Representative images were acquired
211 with a TCS SPE confocal microscope (Leica, Wetzlar, Germany).

212 ***Microvascular reactivity***

213 Isolated microvessels from fresh omentum biopsies were cleaned free of fat and
214 connective tissue under a light microscope and later mounted as ring preparations on a
215 small vessel myograph (DMT, Denmark), as previously described (17). The passive
216 tension and internal diameter were determined with MyoNorm-4 software (Cibertec), for
217 later subject the arteries to a tension equivalent to 90% of 100 mmHg intramural pressure.
218 Arteries were contracted with 35 mmol/l KCl, and endothelium-dependent and
219 independent relaxation responses were assessed by addition of cumulative concentrations
220 of bradykinin (BK, 0.01 nmol/l to 10 μ mol/l) or sodium nitroprusside (SNP, 1 nmol/l to
221 100 μ mol/l), respectively. In some experiments, mesenteric microvessels were treated
222 with *ex vivo* addition of sDPP4 (200 ng/ml) alone or with pre-treatment with the drugs:
223 linagliptin (100 nmol/l), GB83 (10 μ mol/l), SQ 29,548 (10 μ mol/l), MCC 950 (1 μ mol/l)
224 or anakinra (1 μ g/ml).

225 ***Total RNA isolation and quantitative real-time (qRT)-PCR***

226 For gene expression analysis, total RNA was extracted from frozen visceral AT pieces
227 (30 mg) with NZYol (NZYTech, Lisbon, Portugal). RNA integrity was tested by a
228 NanoDrop 2000 spectrophotometer (ThermoFisher Scientific) and cDNA synthesis was
229 performed using the First-Strand cDNA Synthesis kit (NZYTech), with 500 ng of RNA
230 as template. qRT-PCR reactions were performed with iTaq Universal SYBR Green
231 Supermix (Bio-Rad) on a 7500 Fast Real-Time PCR System (ThermoFisher Scientific)
232 and specific primers against DPP4, p53, p21, p16, NLRP3, IL-1 β and IL1-18 (please see
233 <http://hyper.ahajournals.org>). The relative quantification of gene expression was
234 determined by $2^{-\Delta\Delta C_t}$ method and rRNA *18S* housekeeping gene was used for normalizing.

235 ***Statistical analysis***

236 Data are presented as mean \pm standard error of the mean (SEM) for the indicated number
237 of experiments. Statistical analysis was performed using GraphPad, Prism 8.0.2 software
238 (California, USA). Normality and homoscedasticity were checked for each variable by
239 Shapiro-Wilk and Brown-Forsythe test, respectively. Two-tailed unpaired Student's t-test
240 (parametric variables) or Mann Whitney test (non-parametric variables) was used to
241 determine differences between two groups. One-way analysis of variance (ANOVA)
242 followed by Bonferroni post-hoc test (parametric variables) or Kruskal-Wallis followed
243 by Dunn's multiple comparison test (non-parametric variables) was used to determine
244 differences among more than two groups. Two-way ANOVA was employed to compare
245 two variables when appropriate. For correlations, the Spearman coefficient was
246 determined. A p value ≤ 0.05 was considered statistically significant.

247

248 **Results**

249 ***sDPP4 induces endothelial cell senescence in vitro***

250 In HUVEC primary cultures, human recombinant sDPP4 caused a concentration-
251 dependent increase in the percentage of SA- β -gal positive stained cells (Figures 1A and
252 1B), almost doubling over 24 hours. From $4.39 \pm 0.29\%$ of positive senescent cells in non-
253 stimulated cultures, submaximal stimulation with 200 ng/ml sDPP4 reached $8.54 \pm 0.12\%$
254 SA- β -Gal⁺ cells, and it was the concentration chosen for all subsequent experiments. It
255 should be noted that circulating sDPP4 levels in healthy patients varies in the range of 200
256 to 600 ng/ml (15).

257 sDPP4 also induced DNA damage in HUVEC, as depicted by both an increased
258 expression of the DNA-damage marker γ H2AX (Figure 1D) and the accumulation of

259 DNA damage spots assessed by immunofluorescence. We detected in the sDPP4-treated
260 cultures a higher number of γ H2AX *foci* and TIFs, indicating DNA injury both at non-
261 telomeric and telomeric position (Supplementary figures S1A, S1B, S1C, and S1D).

262 DNA damage is indeed a major stimulus for the activation of cellular alarm
263 mechanisms leading to cessation of the cell cycle and senescence (21). Consistently,
264 sDPP4 induced an increase in the expression of the effector protein for cell cycle arrest
265 p21 (Figures 1E). Moreover, sDPP4 also induced the phosphorylation of the p-65 (Pp65)
266 NF- κ B subunit and the secretion of the pro-inflammatory cytokine IL-6 (Supplementary
267 figures S1E and S1F), which is consistent with the establishment of an active SASP.

268 ***sDPP4 induces endothelial dysfunction ex vivo***

269 Endothelial senescence is itself a promoter of endothelial dysfunction, another hallmark
270 of vascular aging and one of the earliest age-related vascular modifications (22). In this
271 context, we next examined whether sDPP4 affected the functionality and vasodilator
272 properties of human resistance vessels. We used isolated mesenteric microvessels from
273 human omentum biopsies of control non-obese subjects, whose health-related parameters
274 are indicated in Supplementary table S1A.

275 Figure 1F shows the vasorelaxant responses of mesenteric microvessels in response
276 to increasing concentrations of BK (0.01 nmol/l to 10 μ mol/l). We observed that the
277 incubation with sDPP4 (200 ng/ml) impaired the endothelium-dependent relaxation in
278 response to BK (Figure 1F). Indeed, the mean half-maximal effective concentration value
279 (pEC50) significantly decreased in presence of sDPP4 (5.88 ± 0.19) in comparison to
280 control conditions (7.52 ± 0.17), as shown in Supplemental table S1B.

281 ***The PAR2-COX-2-TP axis mediates sDPP4-induced endothelial senescence and*** 282 ***dysfunction***

283 Since sDPP4 can bind PAR2 leading to downstream COX-2 activation (17,23), we
284 assessed whether this pathway was involved in sDPP4-induced senescence and
285 endothelial dysfunction. First, we observed that either the PAR2 antagonist GB83 (10
286 $\mu\text{mol/l}$), the COX-2 blocker celecoxib (3 $\mu\text{mol/l}$), or the TP antagonist SQ 29,548 (10
287 $\mu\text{mol/l}$) were able to attenuate the percentage of SA- β -gal positive stained cells (Figure
288 2A) and γH2AX expression (Figure 2B) in HUVEC treated with sDPP4. In line with these
289 results, the blockade of PAR2 and TP prior to sDPP4 exposure in human isolated
290 microvessels, also prevented the sDPP4-induced endothelial dysfunction (Figure 2C and
291 2D).

292 *sDPP4 activates NLRP3 inflammasome via the PAR2-COX-2-TP axis*

293 Since the overactivation of NLRP3 inflammasome has been involved in the sterile
294 chronic inflammation and inflammaging associated to vascular disease (24), we
295 addressed the capacity of sDPP4 to activate this innate immune response system. In
296 HUVEC, sDPP4 enhanced the levels of the inflammasome components NLRP3, ASC and
297 pro-IL-1 β (Figures 3A, 3B, and 3C).

298 Upon activation, NLRP3 protein oligomerizes and interacts with ASC to assemble
299 into a multiprotein scaffold (ASC-speck) wherein caspase-1 is activated to process pro-
300 IL-1 β and pro-IL-18 into mature forms. Thus, the formation of ASC-speck structures
301 becomes a hallmark of inflammasome activation (25). In our experiments, sDPP4
302 enhanced ASC-speck formation by 2-fold over the basal speck levels, raising from
303 $2.65\pm 0.46\%$ of ASC-specks positive cells in non-treated cultures to $5.38\pm 0.71\%$ after
304 sDPP4 (200 ng/ml) challenge (Figures 3H and 3I). The latter was shown to be abrogated
305 by MCC 950 (1 $\mu\text{mol/l}$), a specific inhibitor of NLRP3 inflammasome assembly (Figures
306 3H and 3I). In addition, sDPP4 significantly increased the ratio of the cleaved form of

307 active caspase-1 versus pro-caspase-1 (Figure 3D), as well as the expression of IL-1 β , the
308 final product underlying NLRP3 inflammasome activation (Figure 3E).

309 Blocking the PAR2-COX-2-TP axis with GB83 (10 μ mol/l), celecoxib (3 μ mol/l),
310 or SQ 29,548 (10 μ mol/l), significantly reduced the capability of sDPP4 to induce NLRP3
311 and IL-1 β expression (Figure 4A and 4B) and ASC-speck formation (Figures 4C and 4D).

312 ***The NLRP3 inflammasome mediates endothelial cell senescence induced by sDPP4***

313 The fact that PAR2-COX-2-TP axis activation by sDPP4 was mediating both cell
314 senescence and the NLRP3 inflammasome activation, suggested a connexion between
315 these latter cellular events. Indeed, the thromboxane (TXA₂) stable analogue U46619 (1
316 μ mol/l) enhanced the expression and the activation of NLRP3 inflammasome
317 (Supplementary figures S2A, S2B, and S2C), as well as the percentage of SA- β -gal⁺ cells
318 by 1.5-fold, and γ H2AX levels (Supplementary figures S2D and S2E), in a TP-dependent
319 manner.

320 Moreover, blocking the NLRP3 inflammasome activation with MCC 950 (1 μ mol/l)
321 or the IL-1 receptors with anakinra (1 μ g/ml) significantly reduced the number of SA- β -
322 gal⁺ cells induced by sDPP4 (200 ng/ml) or by U46619 (1 μ mol/l) (Figures 5A). Similarly,
323 both drugs abolished sDPP4 or U46619-induced γ H2AX expression (Figures 5B).

324 Additionally, both MCC 950 and anakinra prevented the endothelial dysfunction
325 induced by sDPP4 *ex vivo* in isolated human microvessels (Figure 5C and 5D), thus
326 confirming that human endothelial senescence and endothelial dysfunction elicited by
327 sDPP4 were both mediated by a common pathway involving the NLRP3 inflammasome.

328 ***DPP4 inhibitors abolish the detrimental vascular effects of sDPP4 in vitro and ex vivo***

329 We next aimed to identify pharmacological interventions to prevent the
330 detrimental actions of sDPP4 on human endothelial cells or microvessels. To determine

331 the potential therapeutical benefit of DPP4 inhibition, we evaluated the effects of
332 linagliptin, a non-peptidomimetic DPP4 inhibitor within the top-three most used gliptins
333 for the management of type 2 diabetes mellitus. Linagliptin (10 nmol/l) reduced the
334 increase in SA- β -gal positive cells (Figure 1C), γ H2AX and p21 expression (Figures 1D
335 and 1E) induced by sDPP4. We next tested whether the action of gliptins might be
336 mediated by the relative increase of incretins like GLP-1 due to DPP4 inhibition.
337 However, in the presence of the GLP-1 receptor antagonist exendin-(9-39) (1 μ mol/l),
338 linagliptin could still prevent the pro-senescence capacity of sDPP4, while exendin-(9-
339 39) alone did not significantly modify the basal SA- β -Gal⁺ cells in absence of sDPP4
340 (Supplementary figure S1G).

341 In line with a role for the NLRP3 inflammasome in HUVEC senescence,
342 linagliptin abolished the expression of NLRP3 (Figure 3F) and the functional activation
343 of the complex, as evaluated by IL-1 β expression (Figure 3G) and ASC-speck formation
344 (Figure 3H and 3I). In another set of experiments, we address DPP4 inhibition with the
345 experimental peptidomimetic inhibitor K759 (100 nmol/l), observing similar effects than
346 linagliptin (Figures 1C-1E and 3F-3I). Moreover, linagliptin prevented the defective
347 relaxation of human arteries to BK induced by sDPP4 (Figure 1G).

348 *AT content in DPP4 is associated to endothelial dysfunction and inflammaging in* 349 *human obesity*

350 We next aimed to assess the role of sDPP4 and its inhibition in the context of a
351 human disease. Obesity has been acknowledged as a progeric condition in which patients
352 exhibit features of vascular aging such as endothelial dysfunction (26). We studied a
353 cohort of patients (mean age 50 \pm 13 years old, 57% male), classified as non-obese controls
354 without CMD (BMI<30 kg·m⁻²) and obese patients (BMI \geq 30 kg·m⁻²), whose health-
355 related parameters are indicated in Supplementary table S1A.

356 We first observed that the vascular segments from obese patients exhibited a
357 significant impaired endothelium-dependent relaxation as compared to the control non-
358 obese group, with pEC₅₀ values for BK-relaxation of 7.52 ± 0.17 and 6.10 ± 0.16 for non-
359 obese and obese group of patients, respectively (Figure 6A and supplementary tables S1B
360 and S1C). Interestingly, pEC₅₀ values inversely correlated with BMI (Supplementary
361 table S1B). On the contrary, the endothelium-independent relaxations evoked by SNP (1
362 nmol/l to 100 μ mol/l) were similar in both groups (Figure 6B).

363 In the close proximity of the dissected mesenteric microarteries, we determined
364 in the visceral AT the local expression of DPP4, which was significantly higher in the
365 visceral AT explants from obese patients as compared with control non-obese subjects
366 (Figure 6C). We also quantified the visceral AT mRNA expression of the senescence
367 markers p53, p21, and p16, as well as those of the inflammasome-related genes NLRP3,
368 IL-1 β , and IL-18. The heatmap depicted in Figure 6D shows that all these values were
369 higher in obese patients, validating a pro-inflammatory and pro-senescence neighbouring
370 microenvironment around their mesenteric vasculature. Detailed graphs for each marker
371 are supplied in Supplementary figures S3C-S3H.

372 Interestingly, the pEC₅₀ values for the BK responses inversely correlated with DPP4
373 levels of expression in visceral AT from both non-obese and obese patients (Figure 6E),
374 indicating a close association of local DPP4 expression with the loss of functionality in
375 the near vasculature. We thus explored whether the pharmacological blockade of DPP4
376 and its signalling pathways could ameliorate the impaired vascular functionality in the
377 microvasculature from obese patients. Indeed, the pre-incubation with linagliptin (10
378 nmol/l), GB83 (10 μ mol/l), or SQ 29,548 (10 μ mol/l) significantly improved the BK-
379 induced relaxation in microvessels from obese patients bringing it back to values similar
380 to those observed in control non-obese patients (Figures 6F, 6G, and 6H). These

381 treatments had not affected the vascular reactivity responses in control non-obese
382 microarteries (Figures 1G, 2C-D and Supplementary table S1B).

383

384 **Discussion**

385 Accelerated vascular aging is a common feature of most age-associated diseases (2) and
386 an important driver of frailty and disability (22). The progression of obesity and type 2
387 diabetes mellitus shares common hallmarks with aging, so these diseases are now
388 acknowledged as progeric conditions (3,26-28). Although adipokines have been
389 identified as pivotal effectors in several deleterious actions in the vasculature (29,30),
390 evidence about adipokines playing a role in the progression of inflammaging is still very
391 limited. The adipokine sDPP4 was found to be upregulated in type 2 diabetes and obesity
392 patients (13,15), where it triggers detrimental actions in the vasculature and contributes
393 to insulin resistance and atherosclerosis (17,23), yet its contribution to vascular aging has
394 not been established.

395 In the present study, we have demonstrated that sDPP4 directly induces cell
396 senescence in primary cultured human endothelial cells. The endothelium is a main cell
397 layer in the vascular wall as it tightly controls vascular homeostasis (31). The
398 accumulation of endothelial senescent cells disrupts endothelial functionality and impairs
399 its regenerative capacity (7), and also boosts the pro-thrombotic, pro-atherogenic and pro-
400 inflammatory microenvironment that contributes to inflammaging (32). Therefore,
401 understanding the molecular mechanism underneath endothelial senescence is essential
402 to delay vascular disease in CMD and aging.

403 sDPP4 triggered endothelial cell senescence by activation of PAR2, a metabotropic
404 receptor whose activity in the context of CMD has been related to vascular inflammation

405 (33). PAR2 controls vascular tone and coagulation (34,35) and its expression is
406 upregulated in human coronary atherosclerotic lesions (36), and in animal models of
407 obesity (18) and type 2 diabetes (37). Although the mechanism by which sDPP4 may
408 activate PAR2 is not fully elucidated, the fact is that DPP4 contains a high homologous
409 sequence (SLIG region) in its structure that may directly activate PAR2 independently of
410 its protease activity (16,17,38).

411 In vascular smooth muscle cells and endothelial coronary cells, PAR2 stimulation
412 can directly activate COX-2 (18,23). These results are in line with the molecular pathway
413 we hereby describe in HUVEC. In our hands, the blockade of COX-2 or TP receptors,
414 which are activated by COX-2-derived TXA₂, prevented cell senescence induced by
415 sDPP4 via PAR2, thus pointing at TXA₂ behaves as a final effector of sDPP4 pro-
416 senescence effects. In fact, we observed that TXA₂ could induce endothelial senescence
417 by itself, as previously reported in fibroblasts (39). TXA₂ is a potent vasoconstrictor
418 released by activated endothelial cells that may contribute to the pro-thrombotic status in
419 the senescent endothelium. Interestingly, an enhanced vasoconstrictor prostanoid activity
420 has been associated to obesity-associated complications (40). At the same time, aged
421 blood vessels produce increased amounts of COX-derived contractile factors promoting
422 the early onset of endothelial dysfunction (41,42). In this regard, we have also
423 demonstrated here that sDPP4 induces endothelial dysfunction in human mesenteric
424 microarteries, and that PAR2 or TP blockade prevented the impaired endothelium-
425 dependent relaxation induced by sDPP4.

426 We further hypothesized that sDPP4 might serve as a signal to activate the innate
427 immune response NLRP3 inflammasome machinery and the subsequent production of
428 IL-1 β as mediator of sDPP4-induced endothelial senescence and dysfunction. It has been
429 reported that NLRP3 inflammasome over-activation contributes to vascular disease in

430 metabolic syndromes (11,43,44), while its self-activation reinforces endothelial
431 senescence propagation and vascular aging progression (45). In our *in vitro* setting, the
432 PAR2-COX-2-TP sequence would act upstream NLRP3 inflammasome activation
433 triggered by sDPP4. In fact, we revealed TXA₂ as being able to fire NLRP3
434 inflammasome expression and assembly. A former study observed that TP activation in
435 rat pulmonary arteries leads to activation of voltage-gated K⁺ channels causing cellular
436 potassium efflux (46), one well-established mechanism leading to NLRP3 inflammasome
437 canonical activation. However, the detailed mechanism connecting TP and NLRP3
438 inflammasome activation needs further investigation. In any case, both the
439 pharmacological inhibitor of NLRP3 inflammasome assembly MCC 950 and the direct
440 antagonism of IL-1 receptors by anakinra were able to prevent the endothelial dysfunction
441 induced by sDPP4 in human isolated microarteries. Therefore, we conclude that the same
442 molecular pathway, namely the PAR2-COX-2-TP axis followed by NLRP3
443 inflammasome activation, is mediating either endothelial senescence and dysfunction
444 triggered by sDPP4.

445 The adipokine sDPP4 thus appears as a relevant effector of vascular senescence and
446 dysfunction. The relationship between endothelial senescence and endothelial
447 dysfunction has been previously reviewed (47). While mice models of accelerated aging
448 present impaired reactivity responses (48), the pro-inflammatory microenvironment and
449 decreased nitric oxide bioavailability of endothelial senescent cells seems to be
450 compromise vascular function (49).

451 To evaluate the relevance of our hypothesis in a pathological context of disease, we
452 worked with a cohort of obese patients from whom human omentum samples were
453 obtained. The obese patients (mean IMC 39.7±1.74) exhibited higher basal glucose levels
454 and diastolic arterial pressure in comparison to the control non-obese participants,

455 together with an impaired microarterial endothelium-dependent relaxation to BK in
456 comparison to the control group. Importantly, when DPP4 activity or DPP4 downstream
457 signalling was pharmacologically inhibited *ex vivo*, the endothelial dysfunction of the
458 microvessels from obese participants was restored back to the levels of the control group.
459 At this point, we searched for a potential mechanistical explanation in the context of the
460 AT from which the microarteries were isolated. DPP4 was found overexpressed in the
461 visceral AT from obese over non-obese patients, as previously observed (13,15).
462 Furthermore, the visceral AT from obese patients drew a pro-senescent and pro-
463 inflammatory microenvironment, in which DPP4 expression positively correlated with
464 that of senescence-related genes.

465 Thus, DPP4 might emerge as a novel biomarker of AT senescence. In this line, it
466 was previously found upregulated in senescent fibroblasts and lymphocytes (50) and in
467 the aorta of aged versus young rats (51). Here we must consider a limitation of our study
468 due to the scarce human tissue availability, which makes it difficult to establish a cause-
469 effect relationship between DPP4 content in the AT and endothelial dysfunction in the
470 microarteries. Although we could not establish a direct relation between sDPP4-induced
471 endothelial senescence and dysfunction *in vivo*, we do demonstrate that the
472 pharmacological inhibition of DPP4 activity and its downstream pro-senescence pathway
473 reverted the impaired vasorelaxant response in the microarteries from obese patients,
474 without affecting those from control subjects. Moreover, we show that the tissular context
475 is different in the pathological obesity scenario and that a worse endothelial function
476 indicated by pEC50 values is positively associated with BMI, DPP4 expression and the
477 pro-senescence and pro-inflammatory picture in the visceral AT.

478 In line with our *in vitro* results, we propose that sDPP4 coming from visceral AT
479 might act as a direct inducer of local tissue senescence later propagated to the underlying

480 vascular wall. Previous studies indicated that the visceral AT explants from obese patients
481 express and release higher amounts of sDPP4 in comparison to non-obese subjects (15).
482 In addition, circulating DPP4 activity was formerly associated with an impaired skin
483 microcirculation and flow mediated dilation in type 2 diabetes patients (52,53). Further
484 supporting our results, recent *in vitro* studies have revealed the induction of senescence
485 in the bidirectional crosstalk between AT and the vasculature (54,55). Therefore, the
486 accumulation of senescent adipocytes has been related to an obesity-associated low-grade
487 chronic inflammation (56) and insulin resistance (3), while senescent cells ablation and
488 senolytic therapies alleviated the obese-related metabolic alterations (57,58).

489 At this point, we assessed whether DPP4 inhibitors might entail a therapeutic
490 potential against vascular aging. Linagliptin prevented sDPP4-induced endothelial
491 senescence, improving drastically the defective reactivity responses of obese patients'
492 microvessels. Indeed, previous preclinical data have shown that DPP4 inhibitors exert
493 anti-inflammatory, anti-proliferative (23), and anti-senescence effects *in vitro* (59), yet
494 there are few indirect evidences about their *in vivo* implication in the context of aging.
495 Based on our results, the *in vitro* anti-senescence effect of sDPP4 did not rely on an
496 increased bioavailability of incretins. Interestingly, however, gliptins can bind to DPP4
497 in a region in the close proximity with the SLIG sequence and may thus hamper the direct
498 interaction between sDPP4 and PAR2 in endothelial cells (60).

499 Interestingly, it has been reported that linagliptin treatment ameliorates the
500 progression of premature aging phenotype in klotho KO mice, a model of premature aging
501 (61). Besides, obese mice treated with DPP4 inhibitors exhibited greater survival and
502 lifespan (62). Additionally, in elderly type 2 diabetes patients, gliptin treatment improved
503 mild cognitive impairment in subjects with or without Alzheimer's disease (63). In this
504 context, the SAVORO clinical trial (NCT02576288) will evaluate the effect of saxagliptin

505 preserving arterial safety and dysfunction in obese patients without cardiovascular
506 disease. At present, nevertheless, there is not yet evidence of the ability of DPP4 inhibitors
507 to reduce signs of accelerated vascular aging in humans although, based in the present
508 results, gliptins might appear as a promising strategy to preserve and even improve
509 endothelial function and delay vascular inflammaging.

510 **Perspectives**

511 sDPP4 is an AT-derived product whose levels are enhanced in the context of obesity and
512 type 2 diabetes mellitus, where cardiovascular diseases are the main cause of death and
513 disability. In this study, we identified sDPP4 as a relevant contributor both *in vitro* and
514 *ex vivo* to the progression of two major aspects of vascular aging in the context of human
515 obesity, namely endothelial senescence and endothelial dysfunction. It is accepted that
516 preservation of vascular function is essential for a healthy aging and delay of vascular
517 disease. In this line, we have demonstrated that the pharmacological inhibition of DPP4
518 itself, with approved gliptins, or the downstream signalling was able to reverse DPP4
519 effects in the vasculature, recovering normal vascular function in obese patients. Our
520 results suggest that DPP4 and other AT-derived products are new therapeutic targets to
521 tackle vascular inflammaging.

522 **Acknowledgements**

523 None

524 **Sources of Funding**

525 This work was supported by the Plan Nacional de I+D from Spanish Ministry of Economy
526 [grant numbers SAF2017-84776-R and PID2020-115590RB-100/AEI/
527 10.13039/501100011033 to CFSF and CP as co-PIs], Boehringer Ingelheim España S.A.
528 (BIESA), the Spanish Ministry of Education FPU-MECD program [grant number
529 FPU16/02612 to IV], the European Social Fund and Comunidad Autónoma de Madrid
530 program [grant numbers PEJ-2018-AI/SAL-9955 and PEJ-2017-AI/SAL-6867 to PD and

531 AR, respectively] and Universidad Autónoma de Madrid FPI-UAM program [grant
532 number SFPI/2016-00981 to ASHL].¹

533 **Data availability**

534 The data that support the findings of this study are available from the corresponding
535 author upon reasonable request.

536 **Author contributions**

537 CP, CFSF and TR conceived the manuscript. CP, CFSF, TR and IV designed the
538 experiments. CP, CFSF, IV and JDE wrote the manuscript. IV performed the senescence,
539 and WB experiments and statistically analysed all the data. SV and AR performed and
540 analysed the vascular reactivity experiments. MP, RC and DGO recruited the patients and
541 collected the omentum biopsies. PD and ASHL performed and analysed the qRT-PCR
542 experiments. All authors approved the final version of the manuscript.

543

544 **References**

545 (1) Donato AJ, Morgan RG, Walker AE, Lesniewski LA. Cellular and molecular biology
546 of aging endothelial cells. *Journal of molecular and cellular cardiology* 2015 Dec;89(Pt
547 B):122-135.

548 (2) Ungvari Z, Tarantini S, Donato AJ, Galvan V, Csiszar A. Mechanisms of Vascular
549 Aging. *Circulation research* 2018;123(7):849-867.

550 (3) Burton D, Faragher R. Obesity and type-2 diabetes as inducers of premature cellular
551 senescence and ageing. *Biogerontology* 2018 Dec;19(6):447-459.

552 (4) Jia G, Aroor AR, Jia C, Sowers JR. Endothelial cell senescence in aging-related
553 vascular dysfunction. *Biochimica et biophysica acta. Molecular basis of disease* 2019 Jul
554 1;1865(7):1802-1809.

555 (5) Erusalimsky JD. Vascular endothelial senescence: from mechanisms to
556 pathophysiology. *Journal of Applied Physiology* 2009 Nov 20;106(1):326-332.

557 (6) He S, Sharpless NE. Senescence in Health and Disease. *Cell* 2017 Jun 1;169(6):1000-
558 1011.

¹ Disclosures: The authors declare that the experiments performed with linagliptin were partly supported by Boehringer Ingelheim.

- 559 (7) Erusalimsky JD, Kurz DJ. Cellular senescence in vivo: Its relevance in ageing and
560 cardiovascular disease. *Experimental Gerontology* 2005;40(8):634-642.
- 561 (8) Franceschi C, Garagnani P, Parini P, Giuliani C, Santoro A. Inflammaging: a new
562 immune–metabolic viewpoint for age-related diseases. *Nature reviews. Endocrinology*
563 2018 Jul 25;14(10):576-590.
- 564 (9) WHO. World Health Statistics 2019. 2019;153(12).
- 565 (10) Ouchi N, Parker JL, Lugus JJ, Walsh K. Adipokines in inflammation and metabolic
566 disease. *Nature reviews. Immunology* 2011 Feb;11(2):85-97.
- 567 (11) Rheinheimer J, de Souza BM, Cardoso NS, Bauer AC, Crispim D. Current role of
568 the NLRP3 inflammasome on obesity and insulin resistance: a systematic review.
569 *Metabolism* 2017;74:1-9.
- 570 (12) Chang L, Garcia-Barrio M, Chen Y. Perivascular Adipose Tissue Regulates Vascular
571 Function by Targeting Vascular Smooth Muscle Cells. *Arteriosclerosis, thrombosis, and*
572 *vascular biology* 2020 May;40(5):1094-1109.
- 573 (13) Sell H, Blüher M, Klötting N, Schlich R, Willems M, Ruppe F, et al. Adipose
574 Dipeptidyl Peptidase-4 and Obesity. *Diabetes Care* 2013 Nov 1;36(12):4083-4090.
- 575 (14) Röhrborn D, Wronkowitz N, Eckel J. DPP4 in Diabetes. *Frontiers in immunology*
576 2015 Jul;6:386.
- 577 (15) Lamers D, Famulla S, Wronkowitz N, Hartwig S, Lehr S, Ouwens DM, et al.
578 Dipeptidyl Peptidase 4 Is a Novel Adipokine Potentially Linking Obesity to the Metabolic
579 Syndrome. *Diabetes* 2011 Jul;60(7):1917-1925.
- 580 (16) Wronkowitz N, Görgens SW, Romacho T, Villalobos LA, Sánchez-Ferrer CF, Peiró
581 C, et al. Soluble DPP4 induces inflammation and proliferation of human smooth muscle
582 cells via protease-activated receptor 2. *Biochimica et biophysica acta* 2014
583 Sep;1842(9):1613.
- 584 (17) Romacho T, Vallejo S, Villalobos LA, Wronkowitz N, Indrakusuma I, Sell H, et al.
585 Soluble dipeptidyl peptidase-4 induces microvascular endothelial dysfunction through
586 proteinase-activated receptor-2 and thromboxane A2 release. *Journal of Hypertension*
587 2016 May;34(5):869-876.
- 588 (18) Indrakusuma I, Romacho T, Eckel J. Protease-Activated Receptor 2 Promotes Pro-
589 Atherogenic Effects through Transactivation of the VEGF Receptor 2 in Human Vascular
590 Smooth Muscle Cells. *Frontiers in pharmacology* 2016;7:497.
- 591 (19) Romacho T, Villalobos LA, Cercas E, Carraro R, Sánchez-Ferrer CF, Peiró C.
592 Visfatin as a novel mediator released by inflamed human endothelial cells. *PloS one* 2013
593 October 10;8(10):e78283.

- 594 (20) Romero A, San Hipólito-Luengo A, Villalobos L, Vallejo S, Valencia I, Michalska
595 P, et al. The angiotensin-(1-7)/Mas receptor axis protects from endothelial cell senescence
596 via klotho and Nrf2 activation. *Aging cell* 2019 Feb 17;:e12913.
- 597 (21) Fumagalli M, Rossiello F, Clerici M, Barozzi S, Cittaro D, Kaplunov JM, et al.
598 Telomeric DNA damage is irreparable and causes persistent DNA-damage-response
599 activation. *Nature cell biology* 2012;14(4):355-365.
- 600 (22) Costantino S, Paneni F, Cosentino F. Ageing, metabolism and cardiovascular
601 disease. *The Journal of physiology* 2016 Apr 15;:594(8):2061-2073.
- 602 (23) Wronkowitz N, Görgens SW, Romacho T, Villalobos LA, Sánchez-Ferrer CF, Peiró
603 C, et al. Soluble DPP4 induces inflammation and proliferation of human smooth muscle
604 cells via protease-activated receptor 2. *Biochimica et biophysica acta* 2014
605 Sep;1842(9):1613.
- 606 (24) Haneklaus M, O'Neil LAJ. NLRP3 at the interface of metabolism and inflammation.
607 2015;265.
- 608 (25) Stutz A, Horvath GL, Monks BG, Latz E. ASC speck formation as a readout for
609 inflammasome activation. *Methods in molecular biology (Clifton, N.J.)* 2013;1040:91-
610 101.
- 611 (26) Salvestrini V, Sell C, Lorenzini A. Obesity May Accelerate the Aging Process.
612 *Frontiers in endocrinology (Lausanne)* 2019;10:266.
- 613 (27) Kalyani RR, Golden SH, Cefalu WT. Diabetes and Aging: Unique Considerations
614 and Goals of Care. *Dia Care Dia Care* 2017;40(4)10.2337/dci17-0005.
- 615 (28) Pérez LM, Pareja-Galeano H, Sanchis-Gomar F, Emanuele E, Lucia A, Gálvez BG.
616 'Adipaging': ageing and obesity share biological hallmarks related to a dysfunctional
617 adipose tissue. *J Physiol J Physiol* 2016;594(12)10.1113/jp271691.
- 618 (29) Freitas Lima LC, Braga VdA, do Socorro de França Silva, Maria, Cruz JdC, Sousa
619 Santos SH, de Oliveira Monteiro, Matheus M, et al. Adipokines, diabetes and
620 atherosclerosis: an inflammatory association. *Frontiers in physiology* 2015;6:304.
- 621 (30) Maresca F, Palma VD, Bevilacqua M, Uccello G, Taglialatela V, Giaquinto A, et al.
622 Adipokines, Vascular Wall, and Cardiovascular Disease. *Angiology* 2015 Jan;66(1):8-
623 24.
- 624 (31) Deanfield JE, Halcox JP, Rabelink TJ. Endothelial Function and Dysfunction:
625 Testing and Clinical Relevance. *Circulation* 2007 Mar 13;:115(10):1285-1295.
- 626 (32) Lagoumtzi SM, Chondrogianni N. Senolytics and senomorphics: Natural and
627 synthetic therapeutics in the treatment of aging and chronic diseases. *Free radical biology*
628 *& medicine* 2021 Aug 01;:171:169-190.

- 629 (33) Kagota S, Maruyama K, McGuire JJ. Characterization and Functions of Protease-
630 Activated Receptor 2 in Obesity, Diabetes, and Metabolic Syndrome: A Systematic
631 Review. *BioMed research international* 2016 Feb 23,;2016:3130496-16.
- 632 (34) Sriwai W, Mahavadi S, Al-Shboul O, Grider JR, Murthy KS. Distinctive G protein-
633 dependent signaling by protease-activated receptor 2 (PAR2) in smooth muscle: feedback
634 inhibition of RhoA by cAMP-independent PKA. *PloS one* 2013;8(6):e66743.
- 635 (35) Zhao P, Metcalf M, Bunnett NW. Biased signaling of protease-activated receptors.
636 *Frontiers in endocrinology (Lausanne)* 2014;5:67.
- 637 (36) Napoli C, De Nigris F, Wallace JL, Tajana G, De Rosa G, Sica V, et al. Evidence
638 that protease activated receptor 2 expression is enhanced in human coronary
639 atherosclerotic lesions. *Journal of Clinical Pathology Journal of Clinical Pathology*
640 2004;57(5)10.1136/jcp.2003.015156.
- 641 (37) Kagota S, Chia E, McGuire JJ. Preserved arterial vasodilatation via endothelial
642 protease-activated receptor-2 in obese type 2 diabetic mice. *British journal of*
643 *pharmacology* 2011 Sep;164(2):358-371.
- 644 (38) Macfarlane SR, Seatter MJ, Kanke T, Hunter GD, Plevin R. Proteinase-activated
645 receptors. *Pharmacology Reviews* 2001 Jun,;53(2):245-282.
- 646 (39) Chien C, Fan S, Lin S, Kuo C, Yang C, Yu T, et al. Glucagon-like peptide-1 receptor
647 agonist activation ameliorates venous thrombosis-induced arteriovenous fistula failure in
648 chronic kidney disease. *Thrombosis and haemostasis* 2014 Nov;112(5):1051-1064.
- 649 (40) Chan P, Liao M, Hsieh P. The Dualistic Effect of COX-2-Mediated Signaling in
650 Obesity and Insulin Resistance. *IJMS IJMS* 2019;20(13)10.3390/ijms20133115.
- 651 (41) Félétou M, Huang Y, Vanhoutte PM. Endothelium-mediated control of vascular
652 tone: COX-1 and COX-2 products. *British Journal of Pharmacology* 2011
653 Oct;164(3):894-912.
- 654 (42) Taddei S, Virdis A, Ghiadoni L, Magagna A, Salvetti A. Cyclooxygenase Inhibition
655 Restores Nitric Oxide Activity in Essential Hypertension. *Hypertension* 1997 Jan
656 01,;29(1):274-279.
- 657 (43) Patel M, Galván-Peña S, Mills EL, Olden R, Triantafilou M, Wolf AI, et al.
658 Inflammasome Priming in Sterile Inflammatory Disease. 2016;23.
- 659 (44) De Nardo D, Eicke. NLRP3 inflammasomes link inflammation and metabolic
660 disease. *Trends in Immunology* 2011;32(8):373-379.
- 661 (45) Romero A, Dongil P, Valencia I, Vallejo S, San Hipólito-Luengo Á, Díaz-Araya G,
662 et al. Pharmacological Blockade of NLRP3 Inflammasome/IL- 1 β -Positive Loop
663 Mitigates Endothelial Cell Senescence and Dysfunction. 202110.14336/AD.2021.0617.

- 664 (46) Yoo HY, Park SJ, Seo E, Park KS, Han J, Kim KS, et al. Role of thromboxane A2-
665 activated nonselective cation channels in hypoxic pulmonary vasoconstriction of rat.
666 *American Journal of Physiology - Cell Physiology* 2012 Jan 01,;302(1):307-317.
- 667 (47) Carracedo J, Ramírez-Carracedo R, Altique M, Ramírez-Chamond R. Endothelial
668 Cell Senescence in the Pathogenesis of Endothelial Dysfunction. In: Lenasi H, editor.
669 *Endothelial Dysfunction - Old Concepts and New Challenges*: IntechOpen; 2018.
- 670 (48) Novella S, Dantas AP, Segarra G, Vidal-Gómez X, Mompeón A, Garabito M, et al.
671 Aging-related endothelial dysfunction in the aorta from female senescence-accelerated
672 mice is associated with decreased nitric oxide synthase expression. *Experimental*
673 *Gerontology* 2013 Nov;48(11):1329-1337.
- 674 (49) Wu C, Zheng L, Wang Q, Hu Y. The emerging role of cell senescence in
675 atherosclerosis. 2020;59(1)10.1515/cclm-2020-0601.
- 676 (50) Kim KM, Noh JH, Bodogai M, Martindale JL, Yang X, Indig FE, et al. Identification
677 of senescent cell surface targetable protein DPP4. *Genes & development* 2017 Aug
678 1,;31(15):1529-1534.
- 679 (51) Chen Z, Yu J, Fu M, Dong R, Tang Y, Xiao J, et al. Dipeptidyl peptidase-4 inhibition
680 improves endothelial senescence by activating AMPK/SIRT1/Nrf2 signaling pathway .
681 *Biochemical Pharmacology* 2020 April;96(1):76.
- 682 (52) Barchetta I, Ciccarelli G, Barone E, Cimini FA, Ceccarelli V, Bertocchini L, et al.
683 Greater circulating DPP4 activity is associated with impaired flow-mediated dilatation in
684 adults with type 2 diabetes mellitus. *Nutrition, Metabolism and Cardiovascular Diseases*
685 2019 Oct;29(10):1087-1094.
- 686 (53) da Silva Júnior, Wellington Santana, Souza, Maria das Graças Coelho de, Nogueira
687 Neto JF, Bouskela E, Kraemer-Aguiar LG. Constitutive DPP4 activity, inflammation, and
688 microvascular reactivity in subjects with excess body weight and without diabetes.
689 *Microvascular Research* 2018 Nov;120:94-99.
- 690 (54) Barinda AJ, Ikeda K, Nugroho DB, Wardhana DA, Sasaki N, Honda S, et al.
691 Endothelial progeria induces adipose tissue senescence and impairs insulin sensitivity
692 through senescence associated secretory phenotype. *Nature communications* 2020 Jan
693 24,;11(1):481.
- 694 (55) Parvizi M, Ryan ZC, Ebtehaj S, Arendt BK, Lanza IR. The secretome of senescent
695 preadipocytes influences the phenotype and function of cells of the vascular wall.
696 *Biochimica et biophysica acta. Molecular basis of disease* 2021 Jan 1,;1867(1):165983.
- 697 (56) Atawia RT, Bunch KL, Toque HA, Caldwell RB, Caldwell RW. Mechanisms of
698 obesity-induced metabolic and vascular dysfunctions. *Frontiers in bioscience (Landmark*
699 *edition)* 2019 Mar 1,;24(5):890-934.
- 700 (57) Palmer AK, Xu M, Zhu Y, Pirtskhalava T, Weivoda MM, Hachfeld CM, et al.
701 Targeting senescent cells alleviates obesity-induced metabolic dysfunction. *Aging cell*
702 2019 Mar 25,;18(3):e12950-n/a.

703 (58) Sierra-Ramirez A, López-Aceituno JL, Costa-Machado LF, Plaza A, Barradas M,
704 Fernandez-Marcos PJ. Transient metabolic improvement in obese mice treated with
705 navitoclax or dasatinib/quercetin. *Aging (Albany, NY.)* 2020 Jun 25;12(12):11337-
706 11348.

707 (59) Bi J, Cai W, Ma T, Deng A, Ma P, Han Y, et al. Protective effect of vildagliptin on
708 TNF- α -induced chondrocyte senescence. *IUBMB life* 2019 Jul;71(7):978-985.

709 (60) Arulmozhiraja S, Matsuo N, Ishitsubo E, Okazaki S, Shimano H, Tokiwa H.
710 Comparative Binding Analysis of Dipeptidyl Peptidase IV (DPP-4) with Antidiabetic
711 Drugs – An Ab Initio Fragment Molecular Orbital Study. *PLoS ONE* PLoS ONE
712 2016;11(11)10.1371/journal.pone.0166275.

713 (61) Hasegawa Y, Hayashi K, Takemoto Y, Cheng C, Takane K, Lin B, et al. DPP-4
714 inhibition with linagliptin ameliorates the progression of premature aging in *klotho*^{-/-}
715 mice. *Cardiovascular diabetology* 2017 Dec 1;16(1):154.

716 (62) Zhu B, Li Y, Xiang L, Zhang J, Wang L, Guo B, et al. Alogliptin improves survival
717 and health of mice on a high-fat diet. *Aging cell* 2019 Apr;18(2):e12883-n/a.

718 (63) Isik AT, Soysal P, Yay A, Usarel C. The effects of sitagliptin, a DPP-4 inhibitor, on
719 cognitive functions in elderly diabetic patients with or without Alzheimer's disease.
720 *Diabetes research and clinical practice* 2017 Jan;123:192-198.

721

722 **Novelty and Significance**

723 *What is new?*

724 • The adipokine sDPP4 induces human endothelial cell senescence *in vitro* and
725 human microvascular endothelial dysfunction *ex vivo* by activation of PAR2-
726 COX-2-TP axis and NLRP3 inflammasome.

727 • Over-expression of DPP4 is associated with a pro-senescence and pro-
728 inflammatory microenvironment in the adipose tissue and a worse endothelial
729 function in obese patients.

730 *What is Relevant?*

731 • Pharmacological blockade of DPP4 and its related signalling drastically improves
732 the *ex vivo* vascular function of obese patients exhibiting hyperglycaemia and
733 hypertension.

734 *Summary*

- 735 • DPP4 is a mediator of accelerated vascular aging.
- 736 • Approved antidiabetic DPP4 inhibitors (gliptins) arise as a promising strategy to
- 737 preserve endothelial function and delay vascular inflammaging.

738

739 **Figure Legends**

740 **Figure 1. sDPP4 induces cell senescence *in vitro* and endothelial dysfunction *ex vivo*.**

741 HUVEC were treated with human recombinant sDPP4 (10-500 ng/ml) for 24h. (A)

742 Representative phase contrast microphotographs (200X magnification) showing SA- β -

743 gal staining. Images were captured with a Nikon DS-U3 camera using the NIS-Element

744 4.50 imaging software. Black arrows indicate SA- β -gal⁺ cells, which (B) were quantified

745 by blind manual scoring after the indicated treatments. (n=3-4, *p<0.05 vs. untreated cells

746 by one-way ANOVA). DPP4 inhibitors linagliptin (10 nmol/l) and K579 (100 nmol/l)

747 were used in presence of the submaximal concentration of sDPP4 (200 ng/ml) selected

748 for further experiments, and (C) SA- β -gal staining (D) γ H2AX and (E) p21 protein levels

749 were determined. Data are expressed as fold over sDPP4-induced levels. Representative

750 blots are shown on top of the corresponding graphs (n=3-13, *p<0.05 vs. untreated cells,

751 #p<0.05 vs. sDPP4 (200 ng/ml)-induced response by one-way ANOVA). In other set of

752 experiments, mesenteric microvessels were isolated from omentum biopsies from control

753 non-obese patients that were exposed to (F) sDPP4 (200 ng/ml) alone or (G) in

754 combination with linagliptin (10 nmol/l) and later submitted to BK (10^{-11} - 10^{-5} mol/l) to

755 evaluate endothelium-dependent relaxation. Values (mean \pm SEM) in contraction curves

756 were calculated as average percentage of KCl 35 mmol/l contraction for all segments (n)

757 coming from pooled patients (p) in each group. The curves were expressed as the

758 percentage of the previous potassium-evoked contraction. (*p<0.05 vs. control untreated

759 segments response, #p<0.05 vs. sDPP4 (200 ng/ml)-induced response by two-way
760 ANOVA). L: linagliptin, K: K579.

761 **Figure 2. PAR2-COX-2-TP axis mediates the sDPP4-induced vascular effects.**

762 HUVEC were exposed to sDPP4 (200 ng/ml) alone or in presence of GB83 (10 μ mol/l),
763 celecoxib (3 μ mol/l), or SQ 29,548 (10 μ mol/l), for later assessment of (A) SA- β -gal
764 staining and (B) γ H2AX protein level expression. In panel A data are presented as fold
765 over the number SA- β -Gal⁺ cells after sDPP4 challenge; in panel B data are expressed as
766 fold over sDPP4-induced levels with representative blots shown on top of the
767 corresponding graph (n=3-11, *p<0.05 vs. untreated cells. #p<0.05 vs. sDPP4 (200
768 ng/ml)-treated cultures levels by one-way ANOVA). Results are expressed as mean \pm
769 SEM (error bars). Isolated human mesenteric microvessels were exposed to sDPP4 (200
770 ng/ml) alone or in combination with (C) GB83 or (D) SQ 29,548, and their relaxing
771 capacity was evaluated by myography. Values (mean \pm SEM) in contraction curves were
772 calculated as average percentage of KCl 35 mmol/l contraction for all segments (n)
773 coming from pooled patients (p) in each group. The curves were expressed as the
774 percentage of the previous potassium-evoked contraction. (*p<0.05 vs. control untreated
775 segments response. #p<0.05 vs. sDPP4 (200 ng/ml)-induced response by two-way
776 ANOVA). G: GB83; C: celecoxib; S: SQ 29,548.

777 **Figure 3. sDPP4 triggers NLRP3 inflammasome activation in HUVEC.** The

778 expression of NLRP3 inflammasome components (A) NLRP3 (B) ASC and (C) pro-IL-
779 1 β were determined by western blot in total cell lysates after sDPP4 (200 ng/ml) challenge
780 for 24h. As indicative of NLRP3 inflammasome activation, (D) caspase-1 activation
781 (represented as pro-caspase-1 (p45) versus cle-caspase-1 (p10) fragment expression) and
782 (E) mature IL-1 β expression were validated by western blot. In some experiments,
783 HUVEC were treated with linagliptin (10 nmol/l) or K579 (100 nmol/l) in presence of

784 sDPP4 and **(F)** NLRP3 and **(G)** IL-1 β protein expression were evaluated. For panels A-
785 G, representative blots are shown on top of corresponding graphs (n=3-12, *p<0.05 vs.
786 untreated cells by unpaired t-test or Mann Whitney test). **(H)** The percentage of ASC-
787 specks⁺ cells was quantified under a fluorescence microscope (n=5-10, *p<0.05 vs.
788 untreated cells, #p<0.05 vs. sDPP4 (200 ng/ml)-treated cultures levels by one-way
789 ANOVA). **(I)** ASC-speck visualization by indirect immunofluorescence after 24h
790 challenge with sDPP4 (200 ng/ml) alone or in presence of MCC950 (1 μ mol/l), linagliptin
791 (10 nmol/l) or K579 (100 nmol/l). Confocal representative photographs (630X
792 magnification) where white arrowheads indicate the location of toroidal-shaped ASC
793 specks. Specific antibody against ASC (red) was used, while cell nuclei were
794 counterstained with DAPI (blue). Images were captured with a TCS SPE confocal
795 microscope. Results are shown as mean \pm SEM (error bars). L: linagliptin, K: K579.

796 **Figure 4. sDPP4-induced NLRP3 inflammasome activation is mediated by PAR2-**
797 **COX-2-TP axis.** **(A)** NLRP3 and **(B)** mature IL-1 β protein levels expression were
798 detected by western blot in total cell lysates of HUVEC exposed to sDPP4 (200 ng/ml)
799 alone or in combination with GB83 (10 μ mol/l), celecoxib (3 μ mol/l) or SQ 29,548 (10
800 μ mol/l). Data are represented as fold increase of each protein expression levels in sDPP4-
801 treated cells. Representative blots are shown on top of the corresponding graphs (n=4-8,
802 p<0.05 vs. untreated cells, #p<0.05 vs. sDPP4 (200 ng/ml)-treated cultures levels by one-
803 way ANOVA). ASC-specks⁺ cells were detected by indirect immunofluorescence in
804 presence of the aforementioned treatments. **(C)** Percentage of ASC-specks positive cells
805 was quantified by scoring under a fluorescence microscope (n=3-13, *p<0.05 vs.
806 untreated cells. #p<0.05 vs. sDPP4 (200 ng/ml)-treated cultures levels by one-way
807 ANOVA) **(D)** Representative confocal microscopy images (630X magnification) show
808 specific antibody against ASC (red) and cell nuclei counterstained with DAPI (blue).

809 White arrowheads depict the location of toroidal-shaped ASC specks. Images were
810 captured with a TCS SPE confocal microscope. Results are shown as mean \pm SEM (error
811 bars). G: GB83; C: celecoxib; S: SQ 29,548.

812 **Figure 5. NLRP3 inflammasome and its end-product IL-1 β are the final effector of**
813 **sDPP4-induced vascular effects.** HUVEC were exposed to sDPP4 (200 ng/ml) or the
814 TXA₂ stable analogue U46619 (1 μ mol/l) for 24h alone or in combination with MCC 950
815 (1 μ mol/l) or anakinra (1 μ g/ml). **(A)** SA- β -gal⁺ cells were quantified by manual scoring
816 after indicated treatments. Data are represented as fold over the number of senescent cells
817 in non-treated cultures. **(B)** γ H2AX protein levels were determined by western blot in
818 total cell lysates exposed to the aforementioned treatments. A representative blot is shown
819 on top of the graph. Data are expressed as fold over protein levels in non-treated cultures
820 (n=3-7, *p<0.05 vs. untreated cells, #p<0.05 vs. sDPP4 (200 ng/ml), \$p<0.05 vs. U46619
821 (1 μ mol/l) by one-way ANOVA). Isolated human mesenteric microvessels were exposed
822 to sDPP4 (200 ng/ml) alone or in combination with **(C)** MCC 950 or **(D)** anakinra, and
823 their relaxing capacity was evaluated by myography. Values (mean \pm SEM) in contraction
824 curves were calculated as average percentage of KCl 35 mmol/l contraction for all
825 segments (n) coming from pooled patients (p) in each group. The curves were expressed
826 as the percentage of the previous potassium-evoked contraction. *p<0.05 vs. control
827 untreated segments response. #p<0.05 vs. sDPP4 (200 ng/ml)-induced response by two-
828 way ANOVA. Results are shown as mean \pm SEM (error bars). MCC: MCC 950; AK:
829 anakinra.

830 **Figure 6. AT content in DPP4, pro-senescence and pro-inflammatory genes is**
831 **associated to endothelial dysfunction in human obesity.** Mesenteric microvessels were
832 isolated from omentum biopsies from a group of control non-obese (n=13) and obese
833 (n=12) human donors were submitted to crescent concentration of **(A)** BK (10⁻¹¹-10⁻⁵

834 mol/l) or **(B)** SNP (10^{-9} - 10^{-4} mol/l) to evaluate their endothelium-dependent and
835 independent relaxation responses, respectively. **(C)** The local expression of DPP4 in the
836 visceral AT in the close proximity of the microvessels from control vs. obese patients was
837 analysed by qRT-PCR. **(D)** Heatmap summarizing the levels of visceral AT mRNA
838 expression detected by qRT-PCR of pro-senescence markers p53, p21 and p16 and the
839 NLRP3-inflammasome components and products NLRP3, IL-1 β and IL-18, relative to
840 each patient represented by each one of the columns in the graph. Red intensity depicts
841 the level of expression of each gene as fold increase over the expression of pooled non-
842 obese levels and normalized to 18S rRNA levels. **(E)** Linear correlation analysis was
843 performed between pEC50 values for BK relaxation responses and DPP4 mRNA
844 expression in visceral AT. p-value and Spearman coefficient (r_s), are indicated on top of
845 the graph. Obese patients' dissected microvessels were submitted to cumulative
846 concentration of BK in presence or not of the drugs: **(F)** linagliptin, **(G)** GB83 or **(H)** SQ
847 29,548. In panels A, B, E, F and G, the values (mean \pm SEM) in contraction curves were
848 calculated as average percentage of KCl 35 mmol/l contraction for all segments (n)
849 coming from pooled patients (p) in each group. The curves were expressed as the
850 percentage of the previous potassium-evoked contraction, which is indicated in the
851 Supplemental figure S4C. *p<0.05 vs. control (non-obese or obese) untreated segments
852 response. (#p<0.05 vs. sDPP4 (200 ng/ml)-induced response by two-way ANOVA).